Polypharmacology-based Approach for Screening of Traditional Chinese Medicinal extract and Multi-dimensional Targeting Verification

Zhiyong Wu
Northeast Agricultural University
Chunli Xia
Northeast Agricultural University
Ze Wang
Northeast Agricultural University
Jiaxin Bao
Northeast Agricultural University
Rui Li
Northeast Agricultural University
Muhammad Ishfaq
Northeast Agricultural University
Jichang Li (lijichang@neau.edu.cn)
Northeast Agricultural University https://orcid.org/0000-0002-1779-1190

Research

Keywords: Polypharmacology, Traditional Chinese Medicine, Omics, Multi-target, Network pharmacology, Molecular docking

Posted Date: January 13th, 2021

DOI: https://doi.org/10.21203/rs.3.rs-142256/v1

Abstract

Background: Natural products and their unique polypharmacology offer significant advantages for finding novel therapeutics particularly for the treatment of complex diseases. Meanwhile, natural products in traditional Chinese medicine possess drug-like properties. In this study, we used the previously established co-infection model of *Mycoplasma gallisepticum* and *Escherichia coli* as a representative of complex diseases. The multi-omics joint analysis was used to reverse screen TCMs from the Chinese medicinal database and then targeted verification was conducted from multiple dimensions.

Results: The results showed that the Chinese herbal compound screened by the target network played a good therapeutic effect in the case of co-infection. Furthermore, the four methods were performed at gene, protein, and metabolite levels, as well as molecular docking *in vitro* respectively, which were used to verify the multi-target therapeutic effect.

Conclusions: These data suggest that we may provide a new method to validate target combinations of natural products that can be used to optimize their multiple structure-activity relationships to obtain drug-like natural product derivatives. Furthermore, the study could establish a new methodology for the research of Chinese herbal medicinal extract and provide a new multi-target treatment method for the occurrence of co-infection.

Background

Polypharmacology has been widely recognized as a new approach of modern drug discovery [1, 2], which might enable natural products to surpass the use of the traditional single-target drugs in terms of efficiency [3]. Natural products with polypharmacological profiles show a promising prospect for the development of novel therapeutics for various complex diseases [4]. The methods commonly used in polypharmacology include Molecular docking [5, 6], Network-based approaches [7, 8], and Omics-based systems biology approaches [9–11] along with the development of in silico pharmacology [12]. However, unlike pharmacological drugs used in Western medicine, the active components of natural medicines are often not precisely specified [13], which has greatly restricted the development of traditional Chinese medicine (TCM). But more and more research methods on Chinese herbal compounds have been reported in recent years. Pan's study focused on the intervention of Huanglian Decoction in rats with type 2 diabetes mellitus by the methods of network pharmacology and metabolomics [14]. Zhou probed into the effect of Liuwei Dihuang decoction on the neuroendocrine immunomodulation network [15]. In the present study, network pharmacology and systems biology will enable us to deliberately design lead molecules with expected polypharmacology as well as offer opportunities for TCM formula repurposing.

Due to the intensification of commercial poultry production, explosive multiple respiratory infections have become an urgent problem [16]. This co-pathogenesis is characterized by complex interactions between co-infection pathogens and the host [17, 18]. Combined with the previous researches on the co-infection

of *Mycoplasma gallisepticum* (MG) and *Escherichia coli* (*E.coli*) in our laboratory [16, 19, 20], we try to screen a new Chinese medicinal compound (NCMC) with the method of multi-pharmacology and carry out targeted verification. There are many examples of natural products being used in drug discovery efforts that are directed at a wide range of indications beyond their traditional strengths with the development of research technologies [21–23]. Moreover, the complex mechanisms of co-infection were gradually unraveled [24, 25]. However, whether the co-infection can be combined with the complex effects of TCM compounds has never been studied. The study could establish a new methodology for the research of Chinese herbal medicinal extract and provide a new multi-target treatment method for the occurrence of co-infection.

Materials And Methods

Bacterial infection and Experimental groupings

R_{low} strain was obtained from the Harbin Institute of Veterinary Medicine (Chinese Academy of Agricultural Sciences), which was grown in a Modified Hayflicks medium. Escherichia coli O78 was isolated from chickens infected with colibacillosis in our laboratory and cultured in Nutrient Broth (Beijing Aoboxing BIO-TECH Co., Ltd.). The concentration of MG and *E.coli* were 1×10^9 CCU/ml and 10^9 CFU/ml respectively. The detection of the density for MG and *E.coli* were consistent as explained in our previous study [19, 26, 27].

Forty (1 day old) commercial Leghorn chickens were obtained from Chia Chau Chicken Farm (Harbin, Heilongjiang, China) and were assigned randomly to 2 groups namely the Control group and Co-infection group as described in our earlier study [19], Control group: Fed only basal diet; Co-infection group (B): 0.2 ml of MG medium (1×10^9 CCU/ml) was injected into the left caudal thoracic air sac on the 7th day, and 0.1 ml of *E.coli* bacteria (10^9 CFU/ml) was injected intraperitoneally on day 10. On the 13th day, 20 chickens from each group were euthanized using the method of cardiac blood collection. Lung samples in each group were collected for RNA-seq, while the serum samples were collected for non-targeted metabolomics.

Collection of co-infection target genes and construction of TCM-target network

RNA was extracted by Trizol reagent (Invitrogen Inc., Carlsbad, CA) from lung tissue and was utilized to construct the final library (BGISEQ-500 RNA-Seq Library) [19]. DEG-seq method was based on the Poisson distribution (Fold Change > 2 and Adjusted P-value < 0.001) [28, 29]. According to the KEGG annotation results and the official classification, we separately classified the functional and biological pathways of the DEGs. The DEGs from different sub-categories were compared to the STRING database by DIOMAND (www.diamondsearch.org/). To obtain PPI (Protein-protein Interaction) diagram, the gene interactions were obtained by homology with known proteins. The network relations with a score ≥ 300 were screened

out for mapping. After that, the genes with the highest score in PPI results were selected as target genes and used for subsequent network construction.

In the process of network construction, we first collected all the information of the TCMSP database (https://tcmspw.com/tcmsp.php) and got the total network of “TCM-component-target”, which was submitted in Supplementary Material 2. We then put the collected target genes information into the total network for the reverse screening of TCM. The TCM was sorted according to the correlation degree of nodes in the reverse screening network. Furthermore, we classified the TCM based on different functions (Chinese Pharmacopoeia 2015 Edition) and chose the top1 of each classification, including *Isatdis Radix*, *Forsythia Fructus*, *Ginkgo Folium*, *Mori Cortex*, Licorice, and *Radix Salviae*. The details for these single Chinese medicinal herbs and materials and their roles based on TCM theory are listed in Supplementary Material 8. Finally, the TCM-component-target network was established using Cytoscape 3.6.1 software (Bethesda, MD, USA).

Preparation of NCMC

To verify whether the selected compound has a better therapeutic effect and determine the proportion of six herbs. Hence, we had made a treatment experiment based on the uniform design with the methods of pharmacodynamics and minimum inhibitory concentration (MIC). The results showed that the ratio of *Isatdis Radix*, *Forsythia Fructus*, *Ginkgo Folium*, *Mori Cortex*, Licorice, and *Radix Salviae* were 14:7:11:12:5:3 showed effective treatment. The design optimization details of NCMC for the treatment of co-infection was provided in Supplementary materials 7.

Six herbs were purchased from Runhe Chinese medicine processing plant Ltd. Aqueous extract of NCMC was prepared as the following procedure. The medicinal materials were mixed in proportion and were macerated for 1 h with ten folds distilled water (v/w), and then decocted for 1 h, after which the filtrate was collected and the residue was decocted again for 1 h up to six folds (v/w) in distilled water. The filtrates were mixed and condensed and then dried by vacuum-drier at 60 ℃ [30, 31]. The final concentration of the aqueous extract is 1 mg/mL.

UHPLC-QTOF-MS analysis for components quantification

100 μL sample was added to 400 μL of an extracted solution containing 1.25 μg/mL of internal standard which dissolved in water. After 30 s vortex, the samples were sonicated for 10 min in an ice-water bath. After the samples were incubated at -40 ℃ for 1 h, then the sample was centrifuged at 1,2000 rpm for 15 min at 4 ℃. Finally, the supernatant was put in a fresh 2 mL tube and 200 μL was transferred to a fresh glass vial for LC-MS/MS analysis. LC separation was performed on the Nexera UHPLC LC-30A system (SHIMADZU, Japan) with a Waters BEH C18 column (1.7μm*2.1*100 mm, Waters, USA). Mobile phases, water with 0.1% formic acid (A) and acetonitrile (B), were applied with gradient elution and the flow rate was kept at 0.4 mL/min. AB 5600 Triple TOF system (SCIEX, USA) was used to collect primary and secondary MS data based on IDA function under the control software (Analyst TF 1.7 (AB Sciex). Instrument dependent parameters: curtain gas = 35 psi, IonSpray voltage = + 5500 (POS)/-4000 (NEG) V, nebulizer gas = 55 psi, heater gas = 55 psi, source temperature = 550 ℃. The original mass spectrometry

data was imported using Progenesis QI software. The corresponding TCM metabolic database in the compound was established, and the peaks containing MS/MS data were identified by the self-built secondary mass spectrometry database (Biotree Biomedical Technology Co., LTD, China).

NCMC treatment and groupings

A total of 120 White Leghorn chickens was purchased from Chia Chau Chicken Farm (Harbin, Heilongjiang, China), which were divided randomly into 4 groups as follows. Control group (A): Chickens in the CG were fed only with basal diet and inoculated with the culture medium 0.2 mL on day 7 in air sac; Co-infection group (B): The co-infection model was constructed as previously; Co-infection + NCMC administration group (C): The same infection model as mentioned, then treated with the aqueous extract of NCMC, and given orally by gavage. The treatment started on day 13 and continued for 5 days, once a day at a dose of 450 mg/kg; NCMC control group (D): The same dose of NCMC (450 mg/kg) was given orally to chickens by gavage started at day 13 and continued for 5 days. On the 18th day, 20 chickens from each group were euthanized using the method of cardiac blood collection. Lung, tracheal, and serum samples in each group were collected for further analysis.

Microscopic examination of the trachea

First, the tracheal tissues were fixed in 10% formalin, dehydrated, and immersed in the transparent samples of wax, cut into slices (4 μm), stained with hematoxylin and eosin (H & E). Secondly, the tracheal tissues were trimmed into small pieces of 1 mm^3 and fixed overnight in 2.5% glutaraldehyde. They were washed with PBS twice and post-fixed in 1% osmium tetroxide at 4 ℃ for 1 h. Next, the tissues were dehydrated by ethanol series and 100% acetone, embedded in epoxy resins. The ultrathin sections were stained with uranyl acetate and lead citrate and then observed under a GEM-1200ES transmission electron microscope (JEOL Ltd., Tokyo, Japan). Lastly, 1 mm^3 piece of tracheal tissues was also observed by scanning electron microscopy (SEM, SU8010, HITACHI Ltd., Japan).

Joint pathway analysis

16 serum samples of Control and Co-infection groups were examined by the LC-MS system as explained in our previous study [16]. Differentially expressed metabolites (DEMs) were screened in combination with univariate analysis of fold change and q-value. Screening conditions: 1) VIP ≥ 1; 2) fold change ≥ 1.2 or ≤ 0.8333; 3) q-value < 0.05. The DEMs and the previous target gene symbols were imported into the MetaboAnalyst (MetaboAnalyst v4.0), which could simultaneously analyze genes and metabolites of interest within the context of metabolic pathways [32, 33].

Quantitative RT-PCR and western blotting of targets genes

The lung tissue samples were homogenized for 2 min at a low frequency of 65 Hz using an automatic tissue homogenizer machine (Shanghai Jingxin Industrial Development Co., Ltd.). Total RNA was extracted using Trizol reagent (Invitrogen Inc., Carlsbad, CA, United States) and the reverse transcription of cDNA was performed according to the manufacturer's instructions (Takara Biomedical Technology (Beijing) Co., Ltd.). The primer sequences are shown in Table 1. Quantitative RT-PCR was performed to

analyze gene expression using a LightCycler96 (Roche, Basel, Switzerland). Each sample was analyzed in triplicate. The fold change in gene expression was calculated using the △△cycle time (Ct) method after the expression level was normalized with the GAPDH gene taken as an internal standard.

Table 1
Primers used in QRT-PCR analysis of target genes.

Name	Sense Strand/Sense Primer (5'–3')	Antisense Strand/Antisense Primer (5'–3')
NOS2	CAGCTGATTGGGTGTGGAT	TTTCTTTGGCCTACGGGTC
MYC	CCATCATCATCCAGGACTGC	TTGGTAGGTGGCGAGCTTCT
TLR4	TGCCATCCCAACCCAACCACAG	ACACCCACTGAGCAGCACCAA
MMP2	AAACTCACCAGCCTGGGACTAC	CTCCATTCCAAGAATCCGCAATG
VEGFA	CAATTGAGACCCTGGTGGAC	TCTCATCAGAGGCACACAGG
EDN1	GCCAGCCAGAGAGACAAGAA	TGAGCCCAGAGATCTTTTCC
BDKRB1	GTACCCAAGTGTATCGACGCCATC	GCGACAGCCAGGTTCACAAGG
HRH3	GCTCTGCTGATCGCCGTCAC	GCCAGGTTGAGGAGGAAGAAGTTG
CHRM4	AGCCAGGAGGACCACCAAGATG	TGCCCACAATGAACTGCCAGAAC
VAMP2	ATGTCTGCTCCAGCTCCTACCC	CATCCACTTGGGCTTGCGTCTG
IFNG	ACAAGTCAAAGCCGCACATCAAAC	TTTCACCTTCTTCACGCCATCAGG
FOS	ACCTACACCTCCACCTTCGTCTTC	GTTGCTGCTGCTGCCCTTCC

Western blotting was used to measure the related target proteins. Total proteins of lung tissues were extracted by the whole-cell lysis assay and the supernatant protein content was determined using the BCA protein assay kit (Wanlei, Liaoning, China). The membranes were incubated overnight on a shaker at 4 °C with primary antibodies against β-actin (1:5000 dilution), MMP2 (1:500 dilution), TLR4, c-FOS, BDKRB1, VEGFA, and EDN-1 (1:1000 dilution). All the primary antibodies purchased from Bioss Bioscience Inc. (Beijing, China), and species homology included *Gallus gallus*. Secondary anti-mouse and anti-rabbit IgG peroxidase were used for 1 h, and then bound immune-complexes were detected using enhanced chemiluminescence (ECL) detection. The protein bands were analyzed by densitometry using Image J (V 1.42, National Institutes of Health, USA).

Detection of major metabolites by LC-MS

Three key metabolites (Dopamine, γ-Aminobutyric acid, and Leukotriene C4) were obtained from the results of the joint analysis, and the LC-MS method was used for the detection and quantification of targeted metabolites in the anion mode. We first prepared the serum samples and standards for pretreatment by organic precipitation. The information of the three metabolite standards is as follows, Dopamine (BD161397, Bide Pharmatech Ltd., Shanghai, China), γ-Aminobutyric (P10002, APEBIO, USA),

Leukotriene C4 (GC18663, GLPBIO, USA). The mobile phases of Dopamine and γ-Aminobutyric acid were A: 20 mM ammonium formate solution (0.1% formic acid), B: methanol. While, the mobile phases of Leukotriene C4 were: A (0.1% formic water), B (0.1% acetonitrile formate). Then, the Agilent 6490 QQQ mass spectrometer (Agilent Technologies, England) was conducted to obtain the primary and secondary mass spectrometer data based on MRM mode and adopted positive mode. The parameters of the ESI ion source were set as follows: GasTemp: 200℃, GasFlow: 12 L/min, SheathGasFlow: 12 L/min, SheathGas Temp: 350℃. Capillary voltage (VCap): 4000 V. Finally, by using the Mass Hunter Workstation Quantitative (Agilent Technologies, England), the sample concentration was calculated by using the standard product response and corresponding concentration as the standard curve by a single point method.

Predictive models and molecular docking

A total of 12 target proteins were selected considering their key roles in NCMC treatment. According to the results of the joint analysis, these proteins (BDKRB1, CHRM4, EDN1, FOS, HRH3, IFNG, MMP2, MYC, NOS2, TLR4, VAMP2, and VEGFA) were selected for computer simulation of NCMC principal component targeting. The sequence of these five proteins was obtained from the UniProt databases (Universal Protein Resource) [34]. The UniProtKB IDs were as follows: BDKRB1 (Q38Q38), CHRM4 (P17200), EDN1 (F1NWA9), FOS (P11939), HRH3 (F1NVX2), IFNG (P49708), MMP2 (Q90611), MYC (P01109), NOS2 (Q90703), TLR4 (C4PCF3), VAMP2 (A0A1D5PLR5) and VEGFA (P67964).

As the 3D structure of these five proteins (*Gallus gallus*) has not been elucidated yet, the method of comparative modeling was used for their 3D structure [35, 36] to construct the model using the alignment mode. We used PyMol [37] to erase the heteroatoms, water molecules, and inhibitor present in the structure and saved as a PDB file. The 3D structures of the ligand molecule were stored as a Mol2 or SDF file with the help of the TCMSP databases [38] and PubChem (https://pubchem.ncbi.nlm.nih.gov/). The non-bonding interaction of ligand-protease was calculated using Autodock Vina software package [39] for docking analysis. After docking, the interaction of the five proteins and Baicalin with the lowest affinity score for the receptors were selected for further analysis as mentioned in our previous study [40].

Statistical analysis

Data are presented as mean results ± standard deviation (SD). All the experiments were performed in triplicates (n = 3) unless otherwise mentioned. The significance was determined using one-way ANOVA followed by Dunnett's T3 test. The data were analyzed by using the GraphPad Prism (version 5.01). Values with $p < 0.05$ were considered statistically significant. Heatmaps were made by Heatmap Illustrator software (1.03.7). The KEGG classification and the PPI maps were made by the BGI data mining online website (http://report.bgi.com). NCMC component classification diagram was made by RAW graphs (https://rawgraphs.io/).

Results

Transcriptome sequencing of co-infection group and targets screening

In this study, multi-omics analyses were performed on the co-infection model as explained previously [19]. According to the results of RNA-seq, 3,115 DEGs were found between the co-infection and the control groups, including 1,456 genes upregulated and 1,659 genes downregulated. These DEGs were widely distributed in 44 sub-categories in six major categories in the KEGG pathway database, as shown in Fig. 1A. The PPI results in each KEGG classification were submitted in Supplementary Material 1, and the target genes obtained from screening were summarized in Fig. 1A.

Reverse screening of NCMC in TCMSP database

We first collected the entire data of the TCMSP Chinese Medicine Database, which were submitted in Supplementary Material 2. 57 target genes were substituted into the Drug bank database and 25 effective targets were obtained. These 25 targets were brought into the TCMSP total network for the reverse screening of Chinese medicine, and the results showed that 15 targets were matched with the TCMSP database (Reverse network as shown in Supplementary Material 3). Afterward, we sorted the correlation degree of Chinese medicine nodes and selected six high-ranked Chinese medicines according to the classification of Chinese medicines. The six herbs were *Isatdis Radix*, *Forsythia Fructus*, *Ginkgo Folium*, *Mori Cortex*, Licorice, and *Radix Salviae*, and the final "target-component-TCM" network was shown in Fig. 1B.

Component compounds of NCMC aqueous extraction

To clarify the effective ingredients of NCMC, a non-targeted metabolomics method was used to study the aqueous extraction. The results showed that 260 compounds (including positive and negative modes) were detected on the receiver side using UPLC-QTOF-MS/MS. Among them, 85 compounds belong to flavonoids, 64 compounds belong to organic acids, and 17 compounds belong to phenylpropanoids, and so on, as shown in Fig. 2. The complete composition data of NCMC is provided in Supplementary Material 4. Furthermore, the role of the effective ingredients of NCMC was still not clear. Hence, we have screened effective compounds with higher content from the total ion current in both the positive and negative ion modes as shown in Fig. 3. The 2D structure of the ingredients was obtained from the PubChem database (https://pubchem.ncbi.nlm.nih.gov/) and saved as SDF files for subsequent experiments.

Pharmacodynamics’ evaluation of NCMC

Pathological and ultrastructural changes (Fig. 4) were performed to better understand the effects of NCMC treatment on the chicken trachea. In the co-infection group (Fig. 4A), the cilia are exfoliated and there is a proliferation of goblet cells in the upper mucosa. While the cilia are well arranged and there is still a small amount of inflammatory cells infiltrations after NCMC treatment (Fig. 4B). Scanning electron microscopy (SEM) showed that the cilia were significantly more abundant and intact after treatment of co-infection (Fig. 4C and 4D). We can see that cilia rupture, inverted, cytoplasm swelling, matrix electron

density decreased, and the formation of umbrella-like processes to the extracellular in the co-infection group by TEM (Fig. 4E). Although some cilia were shed, the symptoms of the treatment group were significantly improved compared with the co-infection group (Fig. 4F).

Multi-omics joint analysis of co-infection

To explore the metabolic alterations associated with co-infection, we used a UPLC-QTOF-MS/MS-based metabolomics method to examine metabolite alterations in the serum. The non-targeted metabolomics results of the co-infection group showed that there were 245 (58 upregulated and 187 downregulated) and 882 (234 upregulated and 648 downregulated) metabolites in positive and negative modes respectively [16]. Meanwhile, the previous 57 key target genes and differential metabolites were introduced into MetaboAnalyst (v4.0) for further multi-omics joint analysis. The gene-metabolite network is shown in Fig. 5A. Among them, we selected the metabolites and genes with the largest node association degree for subsequent multi-dimensional targeted verification.

Effects of NCMC on the expression of genes and proteins in the lung

According to the gene-metabolite network, 12 genes were screened to investigate the underlying mechanism of the positive effect of NCMC on the target organ, which was used to draw a heatmap for the relationships between the three groups, as shown in Fig. 5B. The heatmap shows that there are different degrees of the eruption of chemokines and mucins secreted by the Co-infection group, except CHRM4, MMP2, and VEGFA. However, half of the genes in the Co-infection + NCMC group showed a significant decrease.

Six key proteins were selected in the network for WB experiments to conduct in-depth research, namely BDKRB1, EDN1, MMP2, TLR4, c-FOS, and VEGFA. From the results of these six proteins (Fig. 5C and 5D), we found that most of the proteins were significantly ($0.01 < p < 0.05$) unregulated in the co-infection group compared to the control groups, except c-FOS. In particular, EDN1, MMP2, and VEGFA showed extremely significant ($p < 0.01$) expressions. After NCMC treatment, the expressions of these target proteins was significantly downregulated in contrast to the Co-infection group. From our results, NCMC significantly modulated the expression of some genes and/or the corresponding proteins, such as MMP2 and TLR4 ($p < 0.01$).

Expression of NCMC on the key metabolites in the serum

We have previously demonstrated that LTC4 in serum could be used as the biomarker for detecting poultry respiratory diseases [16]. Combined with the results of transcriptome-metabonomic network analysis, we, therefore, chose these three metabolites (Dopamine, γ-Aminobutyric acid, and Leukotriene C4) for the detection of the metabolic level. As shown in Fig. 5E and 5F, the expression of three metabolites was up-regulated and extremely significant ($p < 0.01$) between the Control group and the Co-infection group. However, Dopamine and γ-Aminobutyric acid in the NCMC treatment group showed significant reduction ($p < 0.05$) compared with the Co-infection group. Strikingly, the expression of LTC4

showed no significance even after treatment. The original figures (including western blot and UPLC/MS) were provided in Supplementary Material 5.

Molecular docking of effective compounds and target proteins

Based on the results of non-targeted metabolomics of NCMC, a total of 21 effective compounds (including NEG and POS modes) were sorted out. We then performed the molecular docking of the 21 compounds and 12 key proteins. The compounds with the highest docking score absolute value of all 12 key proteins were selected as candidate inhibitors (Docking original figures and docking score details were uploaded as Supplementary Material 6). The optimum ligand-receptor complexes were generated by PyMol and the interaction analysis was analyzed by Protein-Ligand Interaction Profiler [41], as shown in Fig. 6. The most adaptable results of molecular docking showed that BDKRB1 (-6.7 kcal/mol), CHRM4 (-9.3 kcal/mol), EDN1 (-6.3 kcal/mol), FOS (-6.0 kcal/mol), HRH3 (-8.1 kcal/mol), IFNG (-8.7 kcal/mol), MMP2 (-10.1 kcal/mol), MYC (-6.7 kcal/mol), NOS2 (-8.6 kcal/mol), TLR4 (-7.3 kcal/mol), VAMP2 (-5.7 kcal/mol), VEGFA (-8.1 kcal/mol). In view of the overall situation, the docking results reflected the characteristics of NCMC, multi-compound corresponding to single target and single compound corresponding to multi-target. Among them, compounds with the lowest score were Salvianolic acid A (-10.1 kcal/mol), Liquiritigenin (-9.3 kcal/mol), and Isoliquiritigenin (-8.7 kcal/mol) that have the maximum potential to attach to the active site of the target proteins.

Discussion

In this study, we conducted multi-target screening for co-infection of MG and *E.coli* based on omics research and investigated the polypharmacology mechanism of NCMC with multiple components. The whole research were based on the establishment of a co-infection model and the subsequent target screening. According to the previous transcriptome studies on co-infection [19], we obtained a total of 3,115 DEGs and the corresponding KEGG classification. As the previous study showed that oxidative stress transcriptomics and drug discovery approaches could identify and target neurotoxic innate immune populations and lead to the development of selective neuroprotective strategies [42]. However, we hope to screen the representative DEGs from the overall level of *in vivo* studies. Hence, the DEGs from 33 sub-categories of KEGG have carried out PPI analysis respectively as explained in previous studies [43–45]. The screened target genes cannot be applied directly but are matched to the corresponding target according to the Information in the DRUG BANK database.

Hopkins proposed the concept of network pharmacology in 2007, which aims to design a new generation of drugs by incorporating biological networks rather than single target [46]. Network pharmacology-based strategy to predict therapeutic targets of tanshinone I and cryptotanshinone against inflammation, and further to investigate the pharmacological molecular mechanism *in vitro* [47]. For complex diseases, the method of applying network pharmacology was also used to reveal the mechanism of the action of TCM [48, 49]. We collected the whole data of TCMSP for the construction of the total network “TCM-

component-target", and then the targets were substituted into the total network for the reverse screening of TCMs. This method of reverse operation is similar to existing relevant studies [50, 51]. However, this is the first attempt to apply the reverse screening method directly to the TCM network.

After obtaining the order of Chinese herbs, we then selected different categories based on the compatibility theory of Chinese medicines. According to the degree of node correlation, the order was as follows: *Isatdis Radix* (4th, yang tonic) [52], *Forsythia Fructus* (11th, Antipyretic and antidote) [53], *Ginkgo Folium* (5th, Antitussive and antiasthmatic drugs) [54], *Mori Cortex* (3rd, Antitussive and antiasthmatic drugs) [55], Licorice (1st, reinforcing drugs) [56] and *Radix Salviae* (2nd, Drugs with the efficacy of modifying rheological properties of blood) [57]. Aqueous extract of Chinese medicinal compound is the most common method to study compound components [58, 59]. Hence, we sought points that were uniformly scattered on the domain [60, 61], furthermore, we did a multi-nonlinear regression analysis to search for the optimal combination in preliminary experiments. Finally, we obtained the optimal combination of NCMC aqueous extract for subsequent targeted therapy experiments. In the treatment experiment of NCMC aqueous extract for co-infection, we used multiple pathological methods to observe whether a certain curative effect was achieved. Pathological and ultrastructural results showed that the symptoms of co-infection were significantly relieved after treatment, which indicated that NCMC played a significant therapeutic role.

The multi-dimensional validations of targeted therapy were performed at gene, protein, and metabolite levels, as well as computer simulations *in vitro*, respectively. Afterward the joint analysis of transcriptomics and metabolomics, we obtained the network map of key genes and metabolites. Recent studies show that combined metabolomics and transcriptomics analyses provide sensitive approaches to link infection to biological responses [62, 63]. In our study, the first 12 target genes with the highest correlation degree were selected for RT-PCR quantitative detection. The results showed that the expressions of these related genes were reduced after treatment. In particular, various studies have shown that these genes controlled a broad and flexible network in the transcriptome [64, 65]. However, the expression of CHRM4, MMP2, and VEGFA was shown opposite results. We performed western blot to verify protein level expression, which showed similar trends of the six proteins (MMP2, TLR4, c-FOS, BDKRB1, VEGFA, and EDN-1). The quantitative results of targets indicated that the NCMC aqueous extraction can play a multi-target therapeutic role after the reverse screening by network pharmacology.

In the circulation, as the basis of organism phenotypes, metabolites can help us to understand life phenomena more intuitively and effectively and reveal the essence of life [66, 67]. Our previous metabolic results demonstrated that Arachidonic Acid metabolism is activated in co-infection, and it is recommended that LTC4 in serum acts as a biomarker for detecting poultry respiratory diseases [16]. Based on the results of a joint analysis of transcriptomics and metabolomics, dopamine, γ-Aminobutyric acid, and leukotriene C4 were selected for further study. It had been shown that bacterial infection can cause a dopamine burst in the brain and Dopamine activates NF-κB and primes the NLRP3 inflammasome in primary human macrophages [68, 69]. The study also unveiled that γ-Aminobutyric acid, the principal inhibitory neurotransmitter in the brain, has activation functions in the immune system

[70]. These findings are similar to the results of co-infection. Furthermore, the expression of these three metabolites decreased significantly after NCMC treatment.

Finally, to further verify which active components of NCMC aqueous extraction have a multi-target effect, molecular docking was used for *in vitro* analysis. Affinity was the score for the molecular docking, and when the score was lower, the binding affinity was stronger. An affinity < − 7 indicated a stronger binding activity [39]. Our docking results demonstrated the multi-target action of the main active components of the NCMC. In particular, the targeted therapy of Salvianolic acid A, Liquiritigenin, and Isoliquiritigenin could be further investigated. There are even more naturally derived compounds that are either in clinical trials or have shown potential in pre-clinical studies which merit further investigation [71]. In the present study, we used four methods to verify the multi-target therapeutic effect of NCMC extraction. It can be found that NCMC plays a certain role in the expression of key target proteins, and the corresponding key metabolites have also been confirmed.

However, several potential limitations in our experimental and polypharmacology-based approaches should be acknowledged. First, the incomplete known components of natural products curated from publicly available databases limit our approach to predict NCMC extraction for those without known information. Furthermore, the MetaboAnalyst (v 4.0) was used to simultaneously analyze genes and metabolites of interest within the context of metabolic pathways. But only data from humans, mice, and rats are supported currently [32]. Integrating the target network may help to target the growing potential of co-infection genes via indirectly acting on their neighbor proteins in the human interactome. Lastly, the development of TCM should focus on interdisciplinary, combining research from emerging fields after clarifying the material basis. In terms of pharmacodynamics, it is necessary to clarify how NCMC extraction works, such as analyzing the dialectical relationship between "Chinese herbal medicine, probiotics, and intestinal flora".

Conclusion

In summary, the target network for the co-infection was dug through the joint analysis of transcriptomics and metabolomics, and the mapping between the target network and the total TCM network was used to reverse screen TCMs. We started from the network and carried out targeted verification from multiple dimensions to preliminarily reveal the polypharmacological effects of NCMC. These data suggest that we may provide a new method to validate target combinations of natural products, which perhaps to optimize their multiple structure-activity relationships to obtain drug-like natural product derivatives. Furthermore, reverse screening TCMs, which can be used to determine the functional role of TCMs in a wide range of co-infection. Thus, transcriptomics and metabolomics approaches could identify and target co-infection and lead to the development of selective polypharmacology strategies.

Abbreviations

MG, *Mycoplasma gallisepticum*; *E.coli*, *Escherichia coli*; KEGG, Kyoto Encyclopedia of Genes and Genomes; CCU, color change unit; UPLC, ultra-performance liquid chromatography; MS, mass spectrometry; MS/MS, tandem mass spectrometry DEMs, differentially expressed metabolites; DEGs, differentially expressed genes; SD, standard deviation; TCM, traditional Chinese medicine; NCMC, new Chinese medicinal compound; PPI, Protein-protein Interaction; MIC, minimum inhibitory concentration; BDKRB1, B1 bradykinin receptor; CHRM4, Cholinergic receptor muscarinic 4; EDN1, Endothelin-1; FOS, Cellular oncogene fos; HRH3, G protein coupled receptor 97; IFNG, Immune interferon receptor 1; MMP2, Matrix metalloproteinase 2; MYC, Myc proto oncogene protein; NOS2, Nitric Oxide Synthase 2; TLR4, Toll like receptor 4; VAMP2, Vesicle Associated Membrane Protein 2; VEGFA, Vascular endothelial growth factor A.

Declarations

Ethics approval and consent to participate

The present study was conducted under the approval of the Laboratory Animal Ethics Committee of Northeast Agricultural University (Heilongjiang province, China) by Laboratory animal-Guideline for ethical review of animal welfare (GB/T 35892-2018, National Standards of the People's Republic of China).

Consent for publication

Not applicable.

Availability of data and materials

The data analyzed during the current study are available from the corresponding author on reasonable request.

Competing interests

The authors declare that they have no competing interests.

Funding

This work was supported by the National Natural Science Foundation of China (31973005 and 31772801).

Author contributions

ZW and JL designed the study. ZW, JB, IM and RL performed and collected data from experiment and analyzed data. ZW, IM wrote the manuscript. All authors read and approved the final manuscript.

Acknowledgments

We would like to thank Professor Ming Ge of the department of Clinical Veterinary Medicine (Northeast Agricultural University) in our university for his great assistance in screening TCMs. We appreciate Professor Guohua Zhang (Southern Medical University, China) for sharing the whole TCMSP database and providing corresponding guidance. We also thank the Biotree Biotech Co., Ltd. (Shanghai, China) for metabolomics analysis and data interpretation.

References

1. Anighoro A, Bajorath J, Rastelli G. Polypharmacology: challenges and opportunities in drug discovery. Journal of medicinal chemistry. 2014;57(19):7874–87.
2. Kuenzi BM, Remsing Rix LL, Stewart PA, Fang B, Kinose F, Bryant AT, Boyle TA, Koomen JM, Haura EB, Rix U. Polypharmacology-based ceritinib repurposing using integrated functional proteomics. Nat Chem Biol. 2017;13(12):1222–31.
3. Ho TT, Tran QT, Chai CL. The polypharmacology of natural products. Future medicinal chemistry. 2018;10(11):1361–8.
4. Fang J, Liu C, Wang Q, Lin P, Cheng F. In silico polypharmacology of natural products. Brief Bioinform. 2018;19(6):1153–71.
5. Zhong HJ, Lee BR, Boyle JW, Wang W, Ma DL, Hong Chan PW, Leung CH. Structure-based screening and optimization of cytisine derivatives as inhibitors of the menin-MLL interaction, Chemical communications (Cambridge. England). 2016;52(34):5788–91.
6. Liu LJ, Leung KH, Chan DS, Wang YT, Ma DL, Leung CH. Identification of a natural product-like STAT3 dimerization inhibitor by structure-based virtual screening. Cell death disease. 2014;5(6):e1293.
7. Cheng F, Liu C, Jiang J, Lu W, Li W, Liu G, Zhou W, Huang J, Tang Y. Prediction of drug-target interactions and drug repositioning via network-based inference. PLoS Comput Biol. 2012;8(5):e1002503.
8. Wu Z, Lu W, Wu D, Luo A, Bian H, Li J, Li W, Liu G, Huang J, Cheng F, Tang Y. In silico prediction of chemical mechanism of action via an improved network-based inference method. Br J Pharmacol. 2016;173(23):3372–85.
9. Hieronymus H, Lamb J, Ross KN, Peng XP, Clement C, Rodina A, Nieto M, Du J, Stegmaier K, Raj SM, Maloney KN, Clardy J, Hahn WC, Chiosis G, Golub TR. Gene expression signature-based chemical

genomic prediction identifies a novel class of HSP90 pathway modulators, Cancer cell 10(4) (2006) 321 – 30.

10. Savitski MM, Reinhard FB, Franken H, Werner T, Savitski MF, Eberhard D, Martinez Molina D, Jafari R, Dovega RB, Klaeger S, Kuster B, Nordlund P, Bantscheff M, Drewes G. Tracking cancer drugs in living cells by thermal profiling of the proteome. Science. 2014;346(6205):1255784.
11. Birkenstock T, Liebeke M, Winstel V, Krismer B, Gekeler C, Niemiec MJ, Bisswanger H, Lalk M, Peschel A. Exometabolome analysis identifies pyruvate dehydrogenase as a target for the antibiotic triphenylbismuthdichloride in multiresistant bacterial pathogens. J Biol Chem. 2012;287(4):2887–95.
12. Noori HR, Spanagel R. In silico pharmacology: drug design and discovery's gate to the future. In silico pharmacology. 2013;1:1.
13. Tao T, Liu M, Chen M, Luo Y, Wang C, Xu T, Jiang Y, Guo Y, Zhang JH, Natural medicine in neuroprotection for ischemic stroke: Challenges and prospective, Pharmacology & therapeutics (2020) 107695.
14. Pan L, Li Z, Wang Y, Zhang B, Liu G, Liu J. Network pharmacology and metabolomics study on the intervention of traditional Chinese medicine Huanglian Decoction in rats with type 2 diabetes mellitus. J Ethnopharmacol. 2020;258:112842.
15. Zhou W, Cheng X, Zhang Y. Effect of Liuwei Dihuang decoction, a traditional Chinese medicinal prescription, on the neuroendocrine immunomodulation network. Pharmacol Ther. 2016;162:170–8.
16. Wu Z, Chen C, Zhang Q, Bao J, Fan Q, Li R, Ishfaq M, Li J. Arachidonic acid metabolism is elevated in Mycoplasma gallisepticum and Escherichia coli co-infection and induces LTC4 in serum as the biomarker for detecting poultry respiratory disease. Virulence. 2020;11(1):730–8.
17. Yan T, Zhu S, Wang H, Li C, Diao Y, Tang Y. Synergistic pathogenicity in sequential coinfection with fowl adenovirus type 4 and avian orthoreovirus. Veterinary microbiology. 2020;251:108880.
18. Umar S, Delverdier M, Delpont M, Belkasmi SFZ, Teillaud A, Bleuart C, Pardo I, Houadfi ME, Guerin JL, Ducatez MF. Co-infection of turkeys with Escherichia coli (O78) and H6N1 avian influenza virus, Avian pathology. journal of the WVPA. 2018;47(3):314–24.
19. Wu Z, Ding L, Bao J, Liu Y, Zhang Q, Wang J, Li R, Ishfaq M, Li J. Co-infection of Mycoplasma gallisepticum and Escherichia coli Triggers Inflammatory Injury Involving the IL-17 Signaling Pathway, 10(2615) (2019).
20. Bao J, Wu Z, Ishfaq M, Miao Y, Li R, Clifton AC, Ding L, Li J. Comparison of Experimental Infection of Normal and Immunosuppressed Chickens with Mycoplasma gallisepticum. J Comp Pathol. 2020;175:5–12.
21. Ji HY, Liu KH, Kong TY, Jeong HU, Choi SZ, Son M, Cho YY, Lee HS. Evaluation of DA-9801, a new herbal drug for diabetic neuropathy, on metabolism-mediated interaction. Arch Pharm Res. 2013;36(1):1–5.
22. Wang Y, Chen S, Yu O. Metabolic engineering of flavonoids in plants and microorganisms. Appl Microbiol Biotechnol. 2011;91(4):949–56.

23. Langeder J, Grienke U, Chen Y, Kirchmair J, Schmidtke M, Rollinger JM. Natural products against acute respiratory infections: Strategies and lessons learned. J Ethnopharmacol. 2020;248:112298.
24. Bakaletz LO. Viral-bacterial co-infections in the respiratory tract. Curr Opin Microbiol. 2017;35:30–5.
25. Melvin JA, Bomberger JM. Compromised Defenses: Exploitation of Epithelial Responses During Viral-Bacterial Co-Infection of the Respiratory Tract. PLoS pathogens. 2016;12(9):e1005797.
26. Lu Z, Xie D, Chen Y, Tian E, Muhammad I, Chen X, Miao Y, Hu W, Wu Z, Ni H, Xin J, Li Y, Li J. TLR2 mediates autophagy through ERK signaling pathway in Mycoplasma gallisepticum-infected RAW264.7 cells. Molecular immunology. 2017;87:161–70.
27. Ishfaq M, Chen C, Bao J, Zhang W, Wu Z, Wang J, Liu Y, Tian E, Hamid S, Li R, Ding L, Li J. Baicalin ameliorates oxidative stress and apoptosis by restoring mitochondrial dynamics in the spleen of chickens via the opposite modulation of NF-kappaB and Nrf2/HO-1 signaling pathway during Mycoplasma gallisepticum infection. Poultry science. 2019;98(12):6296–310.
28. Wang L, Feng Z, Wang X, Wang X, Zhang X. DEGseq: an R package for identifying differentially expressed genes from RNA-seq data. Bioinformatics. 2010;26(1):136–8.
29. Langmead B, Salzberg SL. Fast gapped-read alignment with Bowtie 2. Nature methods. 2012;9(4):357–9.
30. Kou J, Zhu D, Yan Y. Neuroprotective effects of the aqueous extract of the Chinese medicine Danggui-Shaoyao-san on aged mice. J Ethnopharmacol. 2005;97(2):313–8.
31. Yin JB, Zhou KC, Wu HH, Hu W, Ding T, Zhang T, Wang LY, Kou JP, Kaye AD, Wang W. Analgesic Effects of Danggui-Shaoyao-San on Various "Phenotypes" of Nociception and Inflammation in a Formalin Pain Model. Mol Neurobiol. 2016;53(10):6835–48.
32. Chong J, Wishart DS, Xia J. Using MetaboAnalyst 4.0 for Comprehensive and Integrative Metabolomics Data Analysis. Current protocols in bioinformatics. 2019;68(1):e86.
33. Chong J, Soufan O, Li C, Caraus I, Li S, Bourque G, Wishart DS, Xia J. MetaboAnalyst 4.0: towards more transparent and integrative metabolomics analysis. Nucleic acids research. 2018;46(W1):W486-w494.
34. UniProt Consortium T. UniProt: the universal protein knowledgebase. Nucleic acids research. 2018;46(5):2699.
35. Arnold K, Bordoli L, Kopp J, Schwede T. The SWISS-MODEL workspace: a web-based environment for protein structure homology modelling. Bioinformatics. 2006;22(2):195–201.
36. Guex N, Peitsch MC, Schwede T. Automated comparative protein structure modeling with SWISS-MODEL and Swiss-PdbViewer: a historical perspective, Electrophoresis 30 Suppl 1 (2009) S162-73.
37. Delano WL. The PyMol Molecular Graphics System. 2002;30:442–54.
38. Ru J, Li P, Wang J, Zhou W, Li B, Huang C, Li P, Guo Z, Tao W, Yang Y, Xu X, Li Y, Wang Y, Yang L. TCMSP: a database of systems pharmacology for drug discovery from herbal medicines. J Cheminform. 2014;6:13.

39. Trott O, Olson AJ. AutoDock Vina: improving the speed and accuracy of docking with a new scoring function, efficient optimization, and multithreading. J Comput Chem. 2010;31(2):455–61.
40. Wu Z, Fan Q, Miao Y, Tian E, Ishfaq M, Li J. Baicalin inhibits inflammation caused by coinfection of Mycoplasma gallisepticum and Escherichia coli involving IL-17 signaling pathway. Poultry science. 2020;99(11):5472–80.
41. Salentin S, Schreiber S, Haupt VJ, Adasme MF, Schroeder M. PLIP: fully automated protein-ligand interaction profiler. Nucleic acids research. 2015;43(W1):W443-7.
42. Mendiola AS, Ryu JK, Bardehle S, Meyer-Franke A, Ang KK, Wilson C, Baeten KM, Hanspers K, Merlini M, Thomas S, Petersen MA, Williams A, Thomas R, Rafalski VA, Meza-Acevedo R, Tognatta R, Yan Z, Pfaff SJ, Machado MR, Bedard C, Rios Coronado PE, Jiang X, Wang J, Pleiss MA, Green AJ, Zamvil SS, Pico AR, Bruneau BG, Arkin MR, Akassoglou K. Transcriptional profiling and therapeutic targeting of oxidative stress in neuroinflammation. Nature immunology. 2020;21(5):513–24.
43. Liu C, Liu Y, Liang L, Cui S, Zhang Y. RNA-Seq based transcriptome analysis during bovine viral diarrhoea virus (BVDV) infection. BMC Genomics. 2019;20(1):774.
44. Ji R, Chen Y, Chen W, Wang Y, Gong F, Huang S, Xie R, Zhong M, Liu Z, Yang Z, Fei J, Mao E, Chen E, Identification of Significant Genes and Pathways in Acute Pancreatitis via Bioinformatical Analysis, Digestive diseases and sciences (2020).
45. Ren Y, Li J, Guo L, Liu JN, Wan H, Meng Q, Wang H, Wang Z, Lv L, Dong X, Zhao W, Zeng Q, Ou J. Full-length transcriptome and long non-coding RNA profiling of whiteleg shrimp Penaeus vannamei hemocytes in response to Spiroplasma eriocheiris infection. Fish Shellfish Immunol. 2020;106:876–86.
46. Hopkins AL. Network pharmacology. Nature biotechnology. 2007;25(10):1110–1.
47. Cui S, Chen S, Wu Q, Chen T, Li S. A network pharmacology approach to investigate the anti-inflammatory mechanism of effective ingredients from Salvia miltiorrhiza. Int Immunopharmacol. 2020;81:106040.
48. Wang E, Wang L, Ding R, Zhai M, Ge R, Zhou P, Wang T, Fang H, Wang J, Huang J. Astragaloside IV acts through multi-scale mechanisms to effectively reduce diabetic nephropathy. Pharmacological research. 2020;157:104831.
49. Pan X, Liu Z. Total Synthesis and Antibacterial Activity Evaluation of Griseofamine A and 16- epi-Griseofamine A. Org Lett. 2019;21(7):2393–6.
50. Hou J, Chen W, Lu H, Zhao H, Gao S, Liu W, Dong X, Guo Z. Exploring the Therapeutic Mechanism of Desmodium styracifolium on Oxalate Crystal-Induced Kidney Injuries Using Comprehensive Approaches Based on Proteomics and Network Pharmacology. Front Pharmacol. 2018;9:620.
51. Lauro G, Romano A, Riccio R, Bifulco G. Inverse virtual screening of antitumor targets: pilot study on a small database of natural bioactive compounds. Journal of natural products. 2011;74(6):1401–7.
52. Chan HL, Yip HY, Mak NK, Leung KN. Modulatory effects and action mechanisms of tryptanthrin on murine myeloid leukemia cells. Cell Mol Immunol. 2009;6(5):335–42.

53. Jiao J, Ma DH, Gai QY, Wang W, Luo M, Fu YJ, Ma W. Rapid analysis of Fructus forsythiae essential oil by ionic liquids-assisted microwave distillation coupled with headspace single-drop microextraction followed by gas chromatography-mass spectrometry. Analytica chimica acta. 2013;804:143–50.
54. Lou JS, Xia YT, Wang HY, Kong XP, Yao P, Dong TTX, Zhou ZY, Tsim KWK. The WT1/MVP-Mediated Stabilization on mTOR/AKT Axis Enhances the Effects of Cisplatin in Non-small Cell Lung Cancer by a Reformulated Yu Ping Feng San Herbal Preparation. Front Pharmacol. 2018;9:853.
55. Hou XD, Ge GB, Weng ZM, Dai ZR, Leng YH, Ding LL, Jin LL, Yu Y, Cao YF, Hou J. Natural constituents from Cortex Mori Radicis as new pancreatic lipase inhibitors. Bioorganic chemistry. 2018;80:577–84.
56. Yu Y, Pauli GF, Huang L, Gan LS, van Breemen RB, Li D, McAlpine JB, Lankin DC, Chen SN. Classification of Flavonoid Metabolomes via Data Mining and Quantification of Hydroxyl NMR Signals. Anal Chem. 2020;92(7):4954–62.
57. Kai G, Hao X, Cui L, Ni X, Zekria D, Wu J, WITHDRAWN: Metabolic engineering and biotechnological approaches for production of bioactive diterpene tanshinones in Salvia miltiorrhiza, Biotechnology advances (2014).
58. Duan X, Pan L, Bao Q, Peng D. UPLC-Q-TOF-MS Study of the Mechanism of THSWD for Breast Cancer Treatment. Front Pharmacol. 2019;10:1625.
59. Yang J, Zhu A, Xiao S, Zhang T, Wang L, Wang Q, Han L. Anthraquinones in the aqueous extract of Cassiae semen cause liver injury in rats through lipid metabolism disorder. Phytomedicine. 2019;64:153059.
60. Fang KT, Lin DKJ, Winker P, Zhang Y. Uniform Design: Theory Application Technometrics. 2000;42(3):237–48.
61. Li F, Fan XX, Chu C, Zhang Y, Kou JP, Yu BY, A Strategy for Optimizing the Combination of Active Components Based on Chinese Medicinal Formula Sheng-Mai-San for Myocardial Ischemia, Cellular physiology and biochemistry: international journal of experimental cellular physiology, biochemistry, and pharmacology 45(4) (2018) 1455–1471.
62. Gardinassi LG, Arévalo-Herrera M, Herrera S, Cordy RJ, Tran V, Smith MR, Johnson MS, Chacko B, Liu KH, Darley-Usmar VM, Go YM, Jones DP, Galinski MR, Li S. Integrative metabolomics and transcriptomics signatures of clinical tolerance to Plasmodium vivax reveal activation of innate cell immunity and T cell signaling. Redox Biol. 2018;17:158–70.
63. Go YM, Fernandes J, Hu X, Uppal K, Jones DP. Mitochondrial network responses in oxidative physiology and disease. Free Radic Biol Med. 2018;116:31–40.
64. Sun DP, Lee YW, Chen JT, Lin YW, Chen RM, The Bradykinin-BDKRB1 Axis Regulates Aquaporin 4 Gene Expression and Consequential Migration and Invasion of Malignant Glioblastoma Cells via a Ca(2+)-MEK1-ERK1/2-NF-κB Mechanism, Cancers 12(3) (2020).
65. Jung Y, Yong S, Kim P, Lee HY, Jung Y, Keum J, Lee S, Kim J, Kim J. VAMP2-NRG1 Fusion Gene is a Novel Oncogenic Driver of Non-Small-Cell Lung Adenocarcinoma. Journal of thoracic oncology:

official publication of the International Association for the Study of Lung Cancer. 2015;10(7):1107–11.

66. Bhatt AP, Redinbo MR, Bultman SJ. The role of the microbiome in cancer development and therapy. Cancer J Clin. 2017;67(4):326–44.
67. Cuadrado A, Rojo AI, Wells G, Hayes JD, Cousin SP, Rumsey WL, Attucks OC, Franklin S, Levonen AL, Kensler TW, Dinkova-Kostova AT. Therapeutic targeting of the NRF2 and KEAP1 partnership in chronic diseases, Nature reviews. Drug discovery. 2019;18(4):295–317.
68. Nolan RA, Reeb KL, Rong Y, Matt SM, Gaskill PJJBB. I.-. Health, Dopamine activates NF-κB and primes the NLRP3 inflammasome in primary human macrophages, 2 (2019) 100030.
69. Chertkova EA, Grizanova EV, Dubovskiy IM. Bacterial and fungal infections induce bursts of dopamine in the haemolymph of the Colorado potato beetle Leptinotarsa decemlineata and greater wax moth Galleria mellonella. J Invertebr Pathol. 2018;153:203–6.
70. Fuks JM, Arrighi RB, Weidner JM, Kumar Mendu S, Jin Z, Wallin RP, Rethi B, Birnir B, Barragan A. GABAergic signaling is linked to a hypermigratory phenotype in dendritic cells infected by Toxoplasma gondii. PLoS pathogens. 2012;8(12):e1003051.
71. Mok SW, Wong VK, Lo HH, de Seabra Rodrigues IR, Dias EL, Leung BY, Law L, Liu. Natural products-based polypharmacological modulation of the peripheral immune system for the treatment of neuropsychiatric disorders. Pharmacol Ther. 2020;208:107480.

Figures

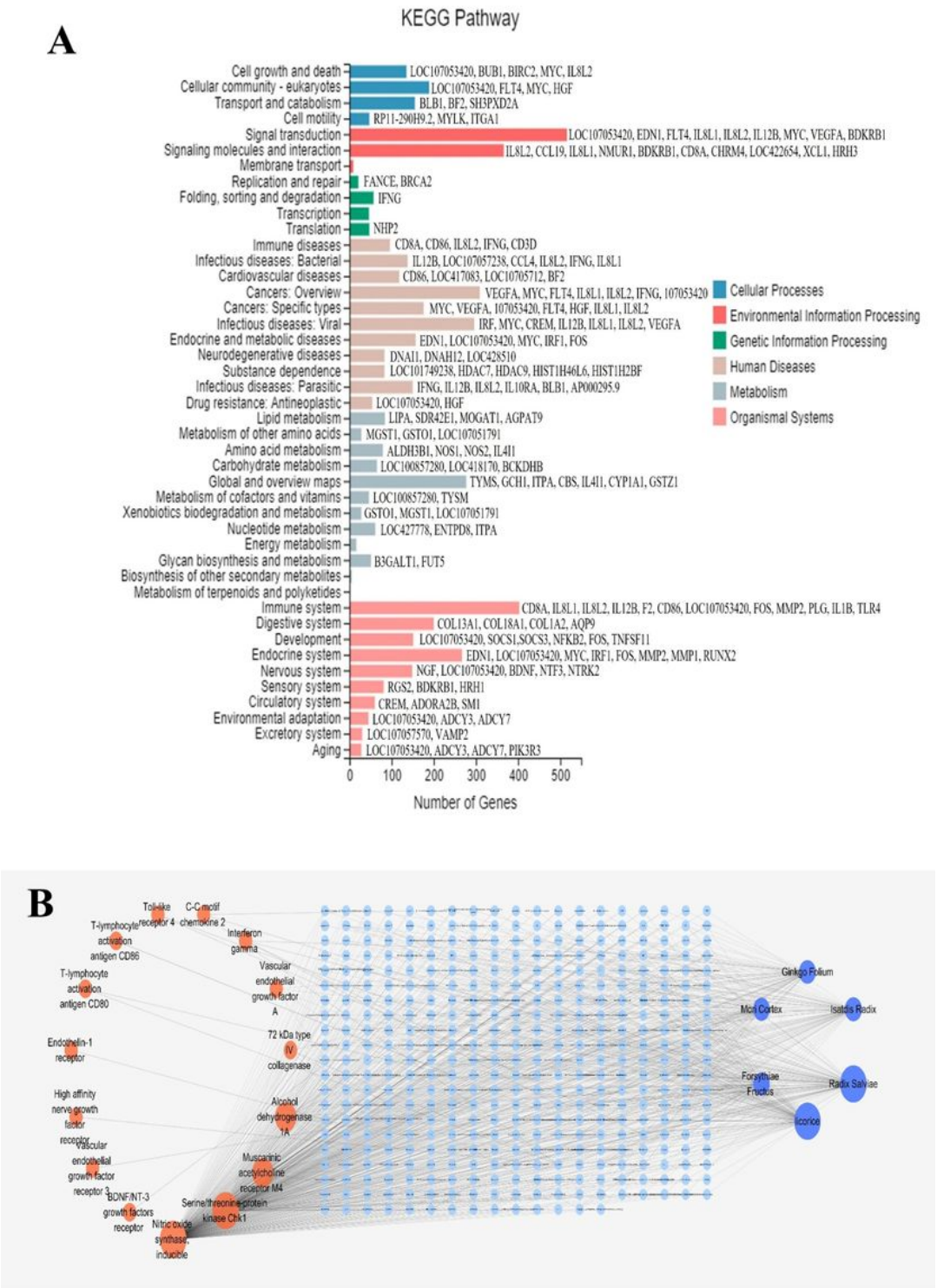

Figure 1

(A) KEGG classification map of DEGs. KEGG categorization of the DEGs in the transcriptome of chicken lung induced by co-infection. The X-axis is the number of genes annotated to a KEGG Pathway classification, and the Y-axis is the KEGG Pathway classification. The gene symbols behind the histogram are the target genes screened by PPI. (B) The predicted "target-component-TCM" network. The orange dots were the effective targets, the dark blue dots were the six Chinese medicines obtained by

reverse screening, and the light blue dots were the components of Chinese medicines. The PPI results in each KEGG classification were submitted in Supplementary Material 1.

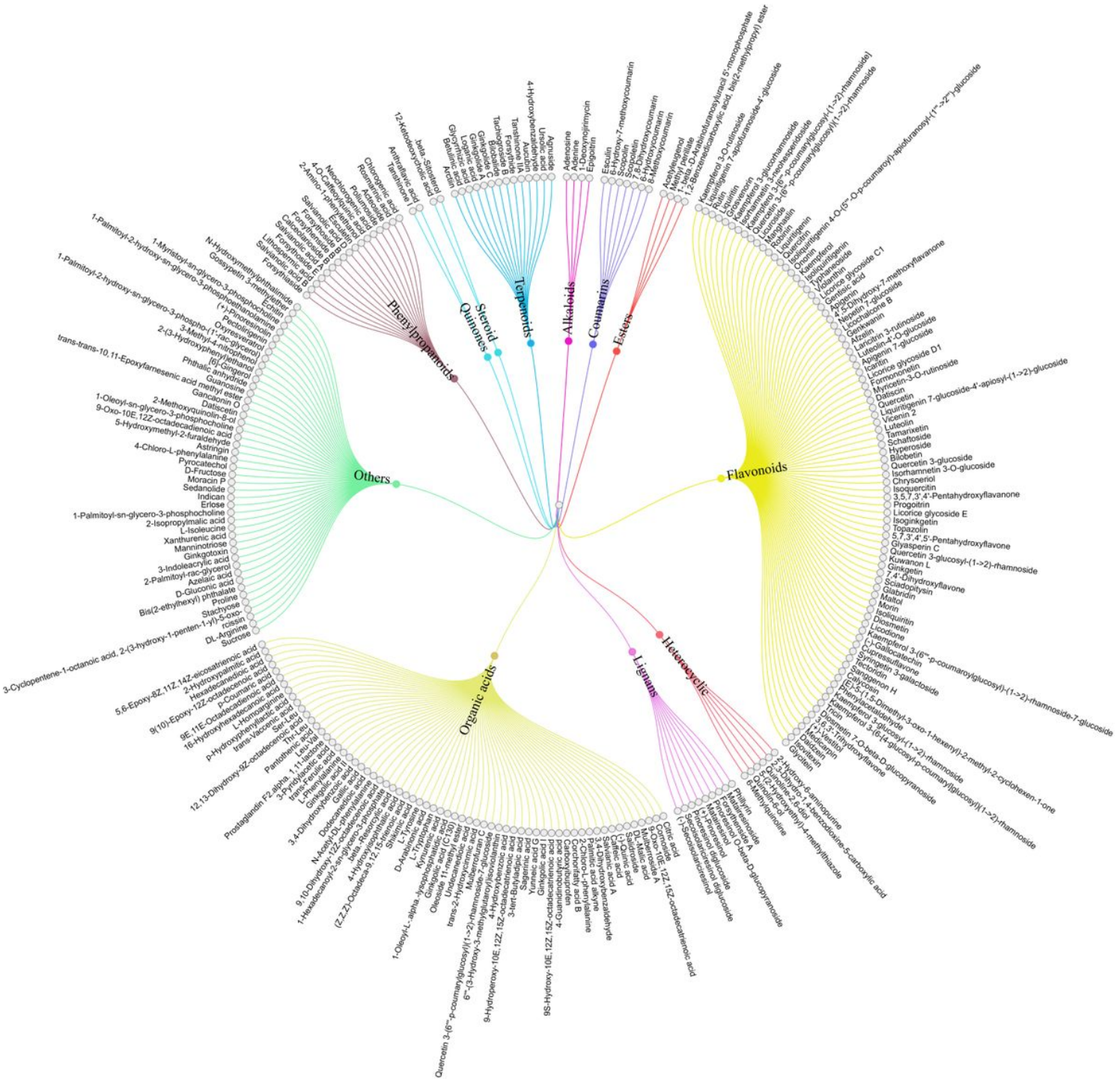

Figure 2

Tree diagram of NCMC aqueous extraction classification. Total 260 compounds belong to 12 categories represented by different colors.

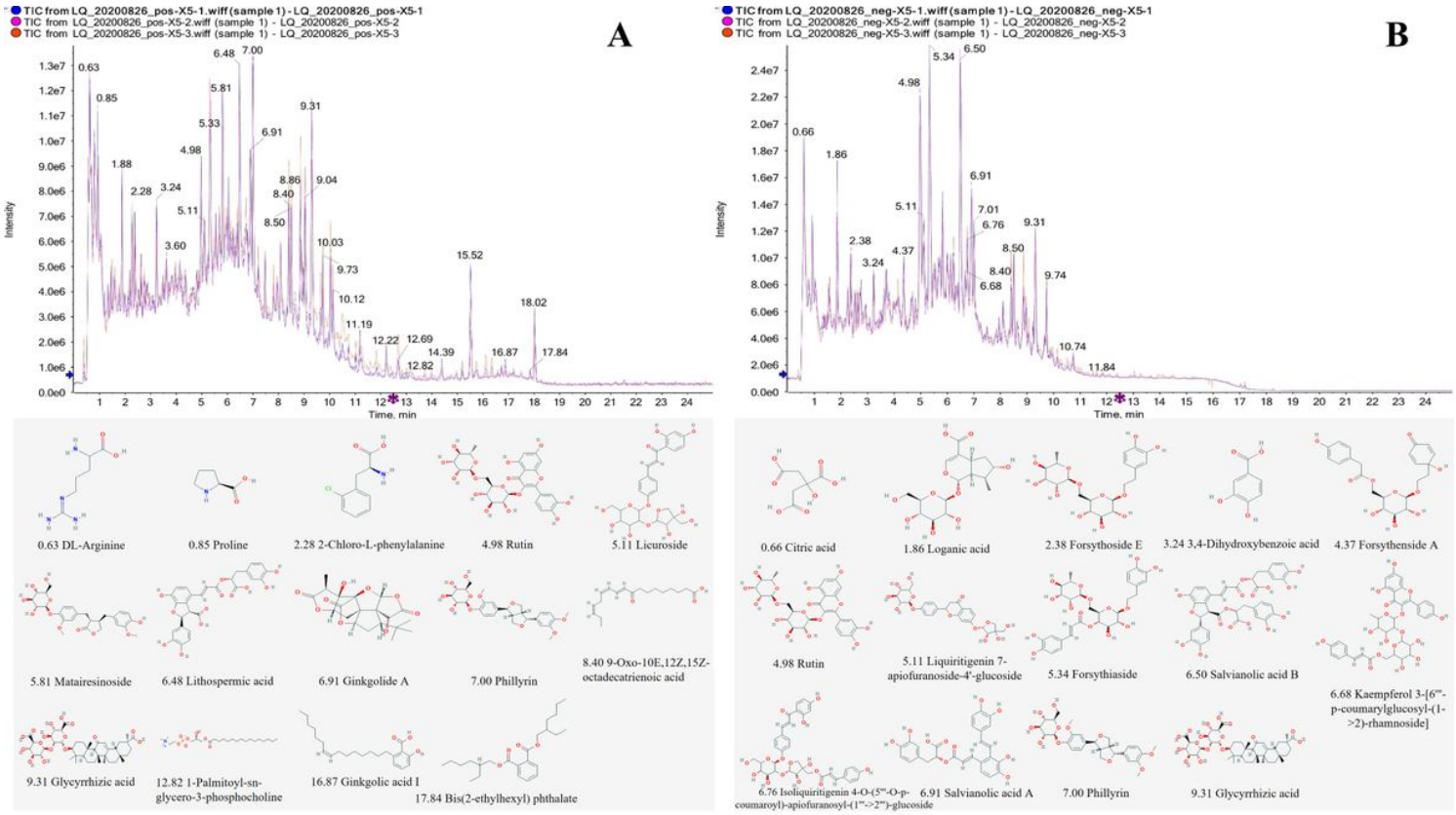

Figure 3

Total ion chromatography diagram in positive (A) and negative (B) ion modes. The 2D structure diagram of main active ingredients as shown below the chromatogram, and the decimal represent the peak times.

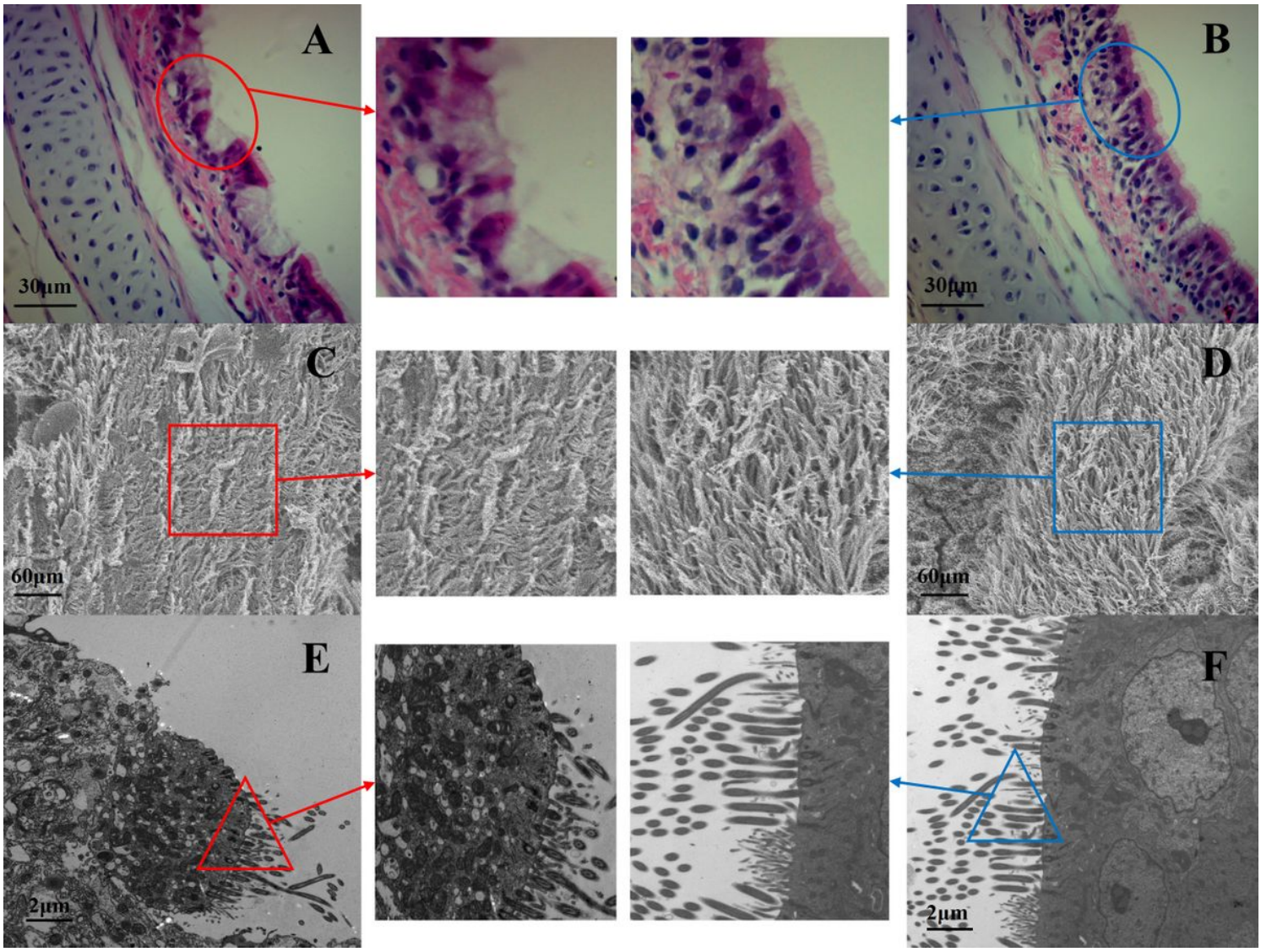

Figure 4

Pathological and ultrastructural changes of NCMC treatment on chicken trachea, (A, C and E from the co-infection group; B, D and F from the NCMC treatment group). Paraffin sections of tracheal tissues from co-infection group and co-infection + NCMC group were stained with hematoxylin-eosin (100×). (A) The red circle shows the cilia are exfoliated and there is a proliferation of goblet cells. (B) The blue circle indicates that the cilia are well arranged and only a small amount of inflammatory cell infiltration. SEM of (C) and (D) at a magnification of 2,500×, and TEM of (E) and (F) at a magnification of 8,000×. (D) The cilia in blue square significantly more abundant and intact after treatment of co-infection (C). (E) The cilia rupture, inverted, cytoplasm swelling, matrix electron density decreased in red triangle of co-infection group. (F) The blue triangle shows some cilia were shed, but the symptoms of the treatment group were significantly improved.

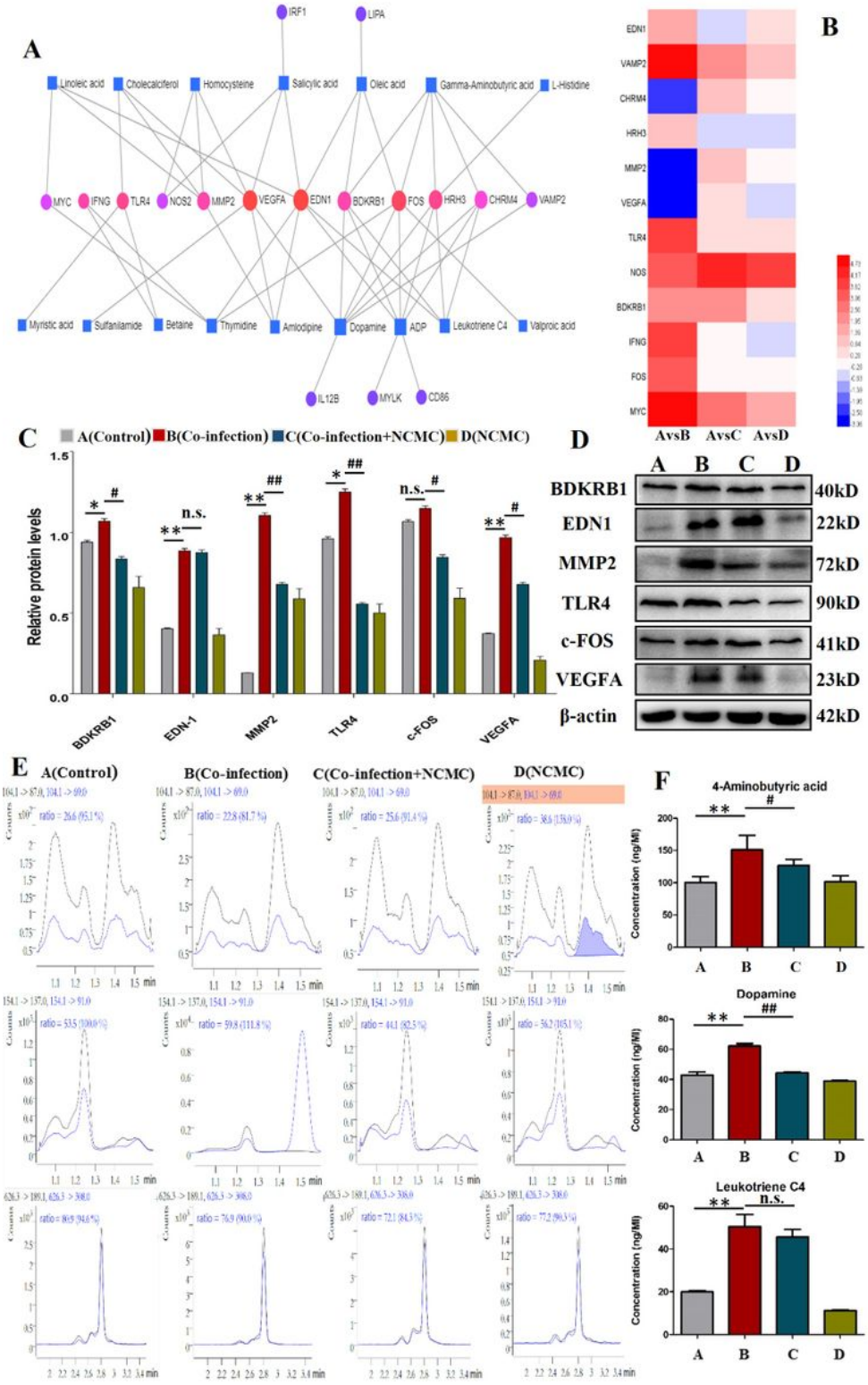

Figure 5

(A) The gene-metabolite joint analysis network. The circles represent genes and the squares represent metabolites. Both the size and the shade of the color indicate the degree from big to small. (B) Heatmap showing the relative gene expression of target genes. A bright red color indicates a stronger up-regulation and a bright blue color indicates a stronger down-regulation in expression. (C) and (D) The protein levels of BDKRB1, EDN1, MMP2, TLR4, c-FOS and VEGFA were measured by western blot. β-actin was used as

an internal control. (E) and (F) Three metabolites (Dopamine, γ-Aminobutyric acid and Leukotriene C4) of chromatogram in four groups by UPLC-MS. Bars represent the mean ± SD. Bars with different superscript letters are significantly different (0.01 < P < 0.05). The original figures (including western blot and UPLC/MS) were provided in Supplementary Material 5.

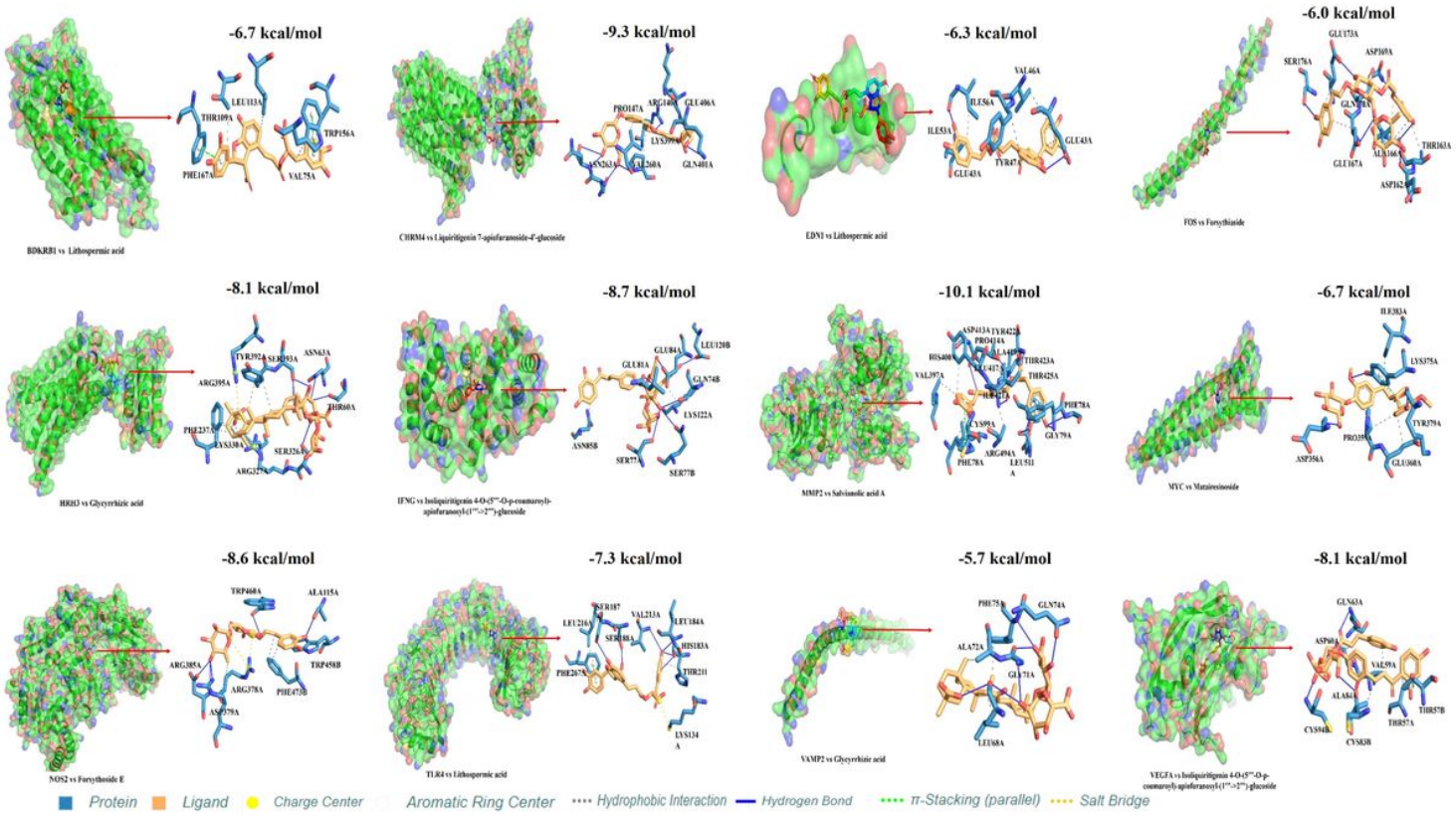

Figure 6

3D models of the optimum ligand and all 12 key proteins (pose predicted by AutoDock Vina; the interaction analysis was analyzed by Protein-Ligand Interaction Profiler). Blue solid line represents Hydrogen Bond, gray dotted line represents Hydrophobic Interactions, the dotted green line represents π-Stacking, the dotted yellow line represents Salt Bridge.

Supplementary Files

This is a list of supplementary files associated with this preprint. Click to download.

- Supplementarymaterials1PPIresults.rar
- Supplementarymaterials4CompoundsofNCMC.xlsx
- Supplementarymaterials7UniformDesign.docx
- Supplementarymaterials8.xlsx